1220 *Inorg. Chem.* **2011**, *50*, 1220–1228
DOI: 10.1021/ic101632v

Inorganic Chemistry
Article

Synthesis and Luminescent Properties of *cis* Bis-*N*-Heterocyclic Carbene Platinum(II) Bis-Arylacetylide Complexes

Yuzhen Zhang, Jai Anand Garg, Clement Michelin, Thomas Fox, Olivier Blacque,* and Koushik Venkatesan*

Institute of Inorganic Chemistry, University of Zürich, Winterthurerstrasse 190, CH-8057, Zürich, Switzerland

Received August 11, 2010

A series of luminescent *N*-heterocyclic carbene platinum(II) complexes, [(pmim)Pt(C≡C−R)$_2$] (R = C_6H_5 (**2**), C_6H_4OMe (**3**), $C_6H_2(OMe)_3$ (**4**), $C_6H_4NMe_2$ (**5**), C_4H_3S (**6**), $C_6H_4C{\equiv}CC_6H_5$ (**7**), 1-pyrenyl (**8**), and C_6H_4F (**9**)), were successfully synthesized using the precursor (pmim)PtI_2, **1** (pmim = 1,1′-dipentyl-3,3′-methylene-diimidazoline-2,2′-diylidene). The X-ray crystal structures of **1**, **4**, **5**, and **7** have been determined. These complexes showed long-lived emission in solution at room temperature. The emission origin of the complexes is tentatively assigned to be from triplet states of predominantly intraligand (IL) character with some mixing of metal-to-ligand charge-transfer (MLCT) character. TD-DFT and DFT calculations have been performed on most of the complexes to ascertain the nature of the excited state. Changes in the alkynyl ligands lead to a change in the absorption and emission maxima seen for these complexes in a potentially predictable way.

Introduction

During the past two decades, heavy metal complexes that display room temperature phosphorescence[1−3]have been actively probed due to their application in phosphorescent organic light-emitting devices (PhOLED).[4,5] Most commonly used heavy metal complexes are based on Pt and Ir.[6−13] In this context, *cis*-platinum σ-acetylide complexes bearing either diimine or phosphine as ancillary ligands (Figure 1) have evoked a lot of recent interest.[14−24] Moreover, devices based on α-diimine bis-(arylacetylide)platinum(II) complexes have also been successfully fabricated and have been shown as promising materials for application in devices.[25] Following the utility of *N*-heterocyclic carbenes as good σ-donating neutral ligands in organometallic chemistry,[26−32] their effect on varying photophysical properties when

*To whom correspondence should be addressed. E-mail: oblacque@aci.uzh.ch (O.B.), venkatesan.koushik@aci.uzh.ch (K.V.).

(1) Bulovic, V.; Gu, G.; Burrows, P. E.; Forrest, S. R.; Thompson, M. E. *Nature* **1996**, *380*, 29–29.
(2) Sun, Y. R.; Giebink, N. C.; Kanno, H.; Ma, B. W.; Thompson, M. E.; Forrest, S. R. *Nature* **2006**, *440*, 908–912.
(3) Yersin, H. *Highly efficient OLEDs with Phosphorescent Materials*; Wiley-VCH: Weinheim, Germany, 2008.
(4) Baldo, M. A.; O'Brien, D. F.; You, Y.; Shoustikov, A.; Sibley, S.; Thompson, M. E.; Forrest, S. R. *Nature* **1998**, *395*, 151–154.
(5) Baldo, M. A.; Thompson, M. E.; Forrest, S. R. *Nature* **2000**, *403*, 750–753.
(6) Brooks, J.; Babayan, Y.; Lamansky, S.; Djurovich, P. I.; Tsyba, I.; Bau, R.; Thompson, M. E. *Inorg. Chem.* **2002**, *41*, 3055–3066.
(7) Furuta, P. T.; Deng, L.; Garon, S.; Thompson, M. E.; Frechet, J. M. J. *J. Am. Chem. Soc.* **2004**, *126*, 15388–15389.
(8) Hirani, B.; Li, J.; Djurovich, P. I.; Yousufuddin, M.; Oxgaard, J.; Persson, P.; Wilson, S. R.; Bau, R.; Goddard, W. A.; Thompson, M. E. *Inorg. Chem.* **2007**, *46*, 3865–3875.
(9) Ma, B. W.; Djurovich, P. I.; Thompson, M. E. *Coord. Chem. Rev.* **2005**, *249*, 1501–1510.
(10) Ma, B. W.; Li, J.; Djurovich, P. I.; Yousufuddin, M.; Bau, R.; Thompson, M. E. *J. Am. Chem. Soc.* **2005**, *127*, 28–29.
(11) You, Y.; Park, S. Y. *Dalton Trans.* **2009**, 1267–1282.
(12) Lamansky, S.; Djurovich, P.; Murphy, D.; Abdel-Razzaq, F.; Lee, H. E.; Adachi, C.; Burrows, P. E.; Forrest, S. R.; Thompson, M. E. *J. Am. Chem. Soc.* **2001**, *123*, 4304–4312.
(13) Tamayo, A. B.; Alleyne, B. D.; Djurovich, P. I.; Lamansky, S.; Tsyba, I.; Ho, N. N.; Bau, R.; Thompson, M. E. *J. Am. Chem. Soc.* **2003**, *125*, 7377–7387.
(14) Hissler, M.; Connick, W. B.; Geiger, D. K.; McGarrah, J. E.; Lipa, D.; Lachicotte, R. J.; Eisenberg, R. *Inorg. Chem.* **2000**, *39*, 447–457.
(15) Miskowski, V. M.; Houlding, V. H.; Che, C. M.; Wang, Y. *Inorg. Chem.* **1993**, *32*, 2518–2524.
(16) Chan, C. W.; Cheng, L. K.; Che, C. M. *Coord. Chem. Rev.* **1994**, *132*, 87–97.
(17) Yam, V. W. W.; Lo, K. K. W.; Wong, K. M. C. *J. Organomet. Chem.* **1999**, *578*, 3–30.
(18) Sacksteder, L.; Baralt, E.; Degraff, B. A.; Lukehart, C. M.; Demas, J. N. *Inorg. Chem.* **1991**, *30*, 2468–2476.
(19) Yam, V. W. W.; Yeung, P. K. Y.; Chan, L. P.; Kwok, W. M.; Phillips, D. L.; Yu, K. L.; Wong, R. W. K.; Yan, H.; Meng, Q. J. *Organometallics* **1998**, *17*, 2590–2596.
(20) Whittle, C. E.; Weinstein, J. A.; George, M. W.; Schanze, K. S. *Inorg. Chem.* **2001**, *40*, 4053–4062.
(21) Pomestchenko, I. E.; Luman, C. R.; Hissler, M.; Ziessel, R.; Castellano, F. N. *Inorg. Chem.* **2003**, *42*, 1394–1396.
(22) Castellano, F. N.; Pomestchenko, I. E.; Shikhova, E.; Hua, F.; Muro, M. L.; Rajapakse, N. *Coord. Chem. Rev.* **2006**, *250*, 1819–1828.
(23) Hua, F.; Kinayyigit, S.; Cable, J. R.; Castellano, F. N. *Inorg. Chem.* **2005**, *44*, 471–473.
(24) Hua, F.; Kinayyigit, S.; Cable, J. R.; Castellano, F. N. *Inorg. Chem.* **2006**, *45*, 4304–4306.
(25) Chan, S. C.; Chan, M. C. W.; Wang, Y.; Che, C. M.; Cheung, K. K.; Zhu, N. Y. *Chem.—Eur. J.* **2001**, *7*, 4180–4190.
(26) Arnold, P. L.; Casely, I. J. *Chem. Rev.* **2009**, *109*, 3599–3611.
(27) Doyle, M. P.; Duffy, R.; Ratnikov, M.; Zhou, L. *Chem. Rev.* **2010**, *110*, 704–724.
(28) Hindi, K. M.; Panzner, M. J.; Tessier, C. A.; Cannon, C. L.; Youngs, W. J. *Chem. Rev.* **2009**, *109*, 3859–3884.

 Published on Web 01/18/2011

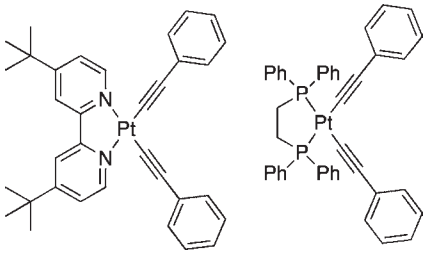

Figure 1. Platinum(II) dialkynyl complexes bearing diimine and bis-phosphine ligands.

compared to diimine or phosphine ligands is of current interest. Developments in bidentate bis-(imidaozolin-2-ylidenes) based metal complexes have been reviewed recently.[33]

Phosphorescence of iridium(III) *N*-heterocyclic carbene and platinum(II) tetracarbene in the ultra/near-UV region and blue region of the spectrum have also been reported.[34−37] While compared to the platinum(II) tetracarbene dicationic complexes, the platinum(II) bis-(imidazolin-2-ylidenes) diiodide complexes do not show any luminescence at RT. It was hypothesized that substitution of the halides with strong field ligands such as alkynes would sufficiently destabilize the metal centered (MC) transition states to higher energies, thereby creating an appropriate metal−ligand environment for effective mixing of singlet−triplet states and radiative relaxation from the triplet manifold. Examples of bis-carbene platinum(II) complexes bearing σ-acetylide ligands *cis* to each other are unprecedented. Together with the aim of achieving emmisivity at RT, an emission tunabilty could also be expected upon varying the electronic properties of the alkyne ligands. Herein, we report the synthesis and spectroscopic properties of a series of platinum(II) bis-(imidazolin-2-ylidenes) bis-(arylacetylide) complexes along with DFT and TD-DFT (time-dependent DFT) calculations to elucidate the photophysical nature of the complexes.

Results and Discussion

Synthesis and Characterization. The preparation of the 1,1′-dipentyl-3,3′-methylene-diimidazoline-2,2′-diylidene (pmim) salt **A** was accomplished in good yield upon reaction of *N*-pentylimidazole with diiodomethane by using a previously reported procedure (see the Supporting Information for details).[36a,37] The bis-carbene Pt(II) diiodide complex **1** (Scheme 1) was obtained in 62% yield following a literature procedure.[36b] Single crystal X-ray

Scheme 1

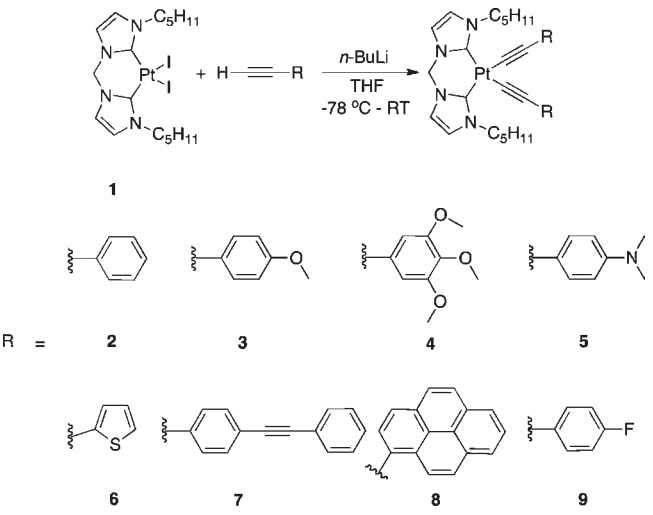

diffraction studies further confirmed the molecular structure of **1**. Our initial attempts to synthesize the diacetylide complex **2** by reaction of **1** with phenylacetylene involving a CuI-catalyzed iodide-to-alkyne metathesis using CH_2Cl_2/$HNiPr_2$ did not proceed in the same fashion as has been reported for the diimine complexes;[25] instead it afforded a mixture of inseparable products. Lithium phenylacetylide in THF was added to complex **1** in THF at −80 °C, and the reaction mixture was stirred at RT for 12 h. Subsequent workup and column chromatography on silica gel gave complex **2** in 54% yield. A total of eight platinum(II) complexes bearing different acetylide ligands were synthesized in moderate to good yields of 36−84% using similar reaction conditions. Scheme 1 shows the general procedure for the synthesis of complexes **2**−**9**.

All of the complexes were fully characterized; the various spectroscopic data (^{1}H NMR, ^{13}C NMR, IR) supported the assignmnent of a square planar platinum(II) center accommodating two *cis*-acetylide and bis-carbene ligands in the coordination sphere. Single crystal X-ray diffraction structures of complexes **4**, **5**, and **7** were also obtained. It is worth noting here that complexes bearing a combination of bidentate *N*-heterocyclic carbene and acetylide ligands are unknown so far. The perspective views of **1**, **4**, **5**, and **7** are shown in Figure 2. As expected, the Pt(II) atom adopted a distorted square planar environment; the Pt−$C_{carbene}$ bond lengths observed in **4**, **5**, and **7** varied between 2.001(11) and 2.041(2) Å and were marginally longer than those of 1.977(4) and 1.984(4) in [Pt(pmim)$_2$I$_2$]. These slight elongations reflect the greater *trans* influence of the phenylacetylide ligands in comparison with the iodide. The bond lengths between the acetylenic carbon atoms in the range 1.194(14)−1.209(15) were similar to those found in platinum(II) diimine bisacetylide complexes.[25] Further, the molecular packing in the crystal structures of these complexes showed no Pt···Pt interactions; the shortest intermolecular Pt···Pt distance was 5.228 Å in **7**. Concentration dependent absorption studies of all of the complexes in CH_2Cl_2 ($c \approx 10^{-6}$−10^{-4} mol dm^{-3}) showed neither a change of the peak maxima nor generation of an additional low energy band, confirming the absence of Pt···Pt interactions in solution and also precluding any excimeric (MMLCT) transitions.

(29) Lin, J. C. Y.; Huang, R. T. W.; Lee, C. S.; Bhattacharyya, A.; Hwang, W. S.; Lin, I. J. B. *Chem. Rev.* **2009**, *109*, 3561–3598.
(30) Mizuhata, Y.; Sasamori, T.; Tokitoh, N. *Chem. Rev.* **2010**, *110*, 3850–3850.
(31) Poyatos, M.; Mata, J. A.; Peris, E. *Chem. Rev.* **2009**, *109*, 3677–3707.
(32) Vougioukalakis, G. C.; Grubbs, R. H. *Chem. Rev.* **2010**, *110*, 1746–1787.
(33) Schuster, O.; Yang, L. R.; Raubenheimer, H. G.; Albrecht, M. *Chem. Rev.* **2009**, *109*, 3445–3478.
(34) Sajoto, T.; Djurovich, P. I.; Tamayo, A.; Yousufuddin, M.; Bau, R.; Thompson, M. E.; Holmes, R. J.; Forrest, S. R. *Inorg. Chem.* **2005**, *44*, 7992–8003.
(35) Unger, Y.; Meyer, D.; Strassner, T. *Dalton Trans.* **2010**, *39*, 4295–4301.
(36) (a) Unger, Y.; Zeller, A.; Taige, M. A.; Strassner, T. *Dalton Trans.* **2009**, 4786–4794. (b) Ahrens, S.; Strassner, T. *Inorg. Chim. Acta* **2006**, *359*, 4789–4796.
(37) Unger, Y.; Zeller, A.; Ahrens, S.; Strassner, T. *Chem. Commun.* **2008**, 3263–3265.

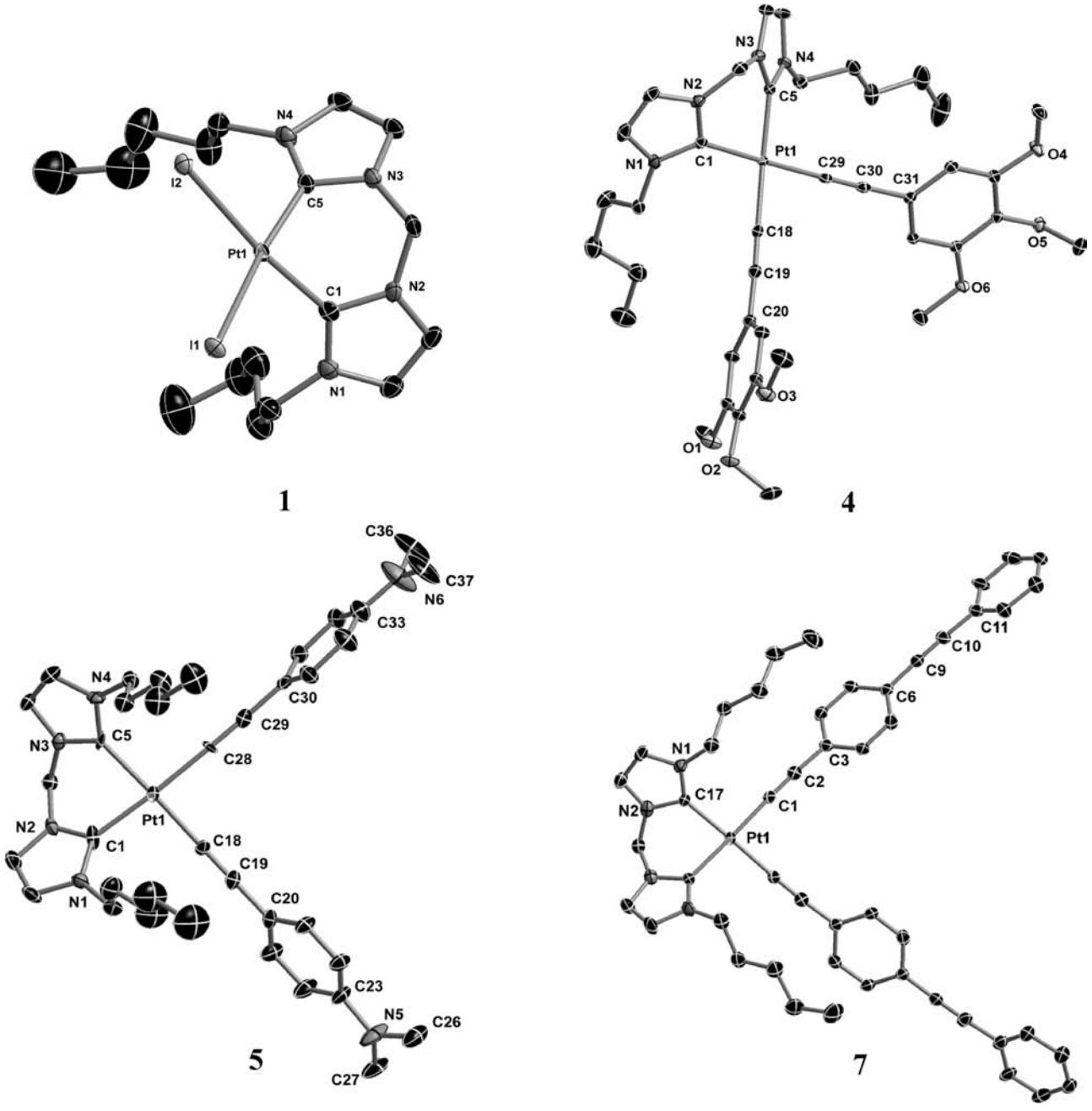

Figure 2. Molecular structures of **1** (top left), **4** (top right), **5** (bottom left), and **7** (bottom right) with a selective atomic numbering scheme. Thermal ellipsoids are drawn at the 30% probability level. Hydrogen atoms and dichloromethane solvent molecules are omitted for clarity.

Photophysical Properties. Figure 3 shows the absorption and emission spectra for complexes **2**−**7** and **9**; for clarity, the absorption spectrum of **8** is shown in the Supporting Information (Figure S3). The dependence of the absorption maxima at *ca.* 325 nm in relation to the acetylide ligands was studied. While the difference in the absorption maxima is barely discernible for **2** and **9**, the band exhibits a significant shift to lower energies for compounds **3**−**8**. Moreover, this systematic bathochromic shift was in line with the increasing electron donating nature of the acetylide ligands (F < H < OMe < $(OMe)_3$ < NMe_2). In addition to this phenomenon, a similar trend was observed with an increase in π-conjugation (**6** < **7** < **8**). The band around 325 nm in the absorption spectra of the complexes showed slight solvatochromic behavior along with the other higher energy bands, which corresponds to the carbene ligand and acetylide-based intraligand transitions (ILCT; see Figure S1 in the Supporting Information). As the electron donating nature of arylacetylide increases, it is expected that the energies of nonbonding and weakly π bonding metal orbitals will increase, leading to the observed red shifts in the complexes.[14]

The RT emissions of all compounds were broad and structureless, while the 77 K spectrum for these compounds showed resolvable vibronic components of the emission (see the Supporting Information). The influence of acetylide variation on the emission energies is evident from Table 1. The extent of observed shifts is greater than those seen in the absorption spectra with trends that are exactly similar. The observed bathochromic trends, both

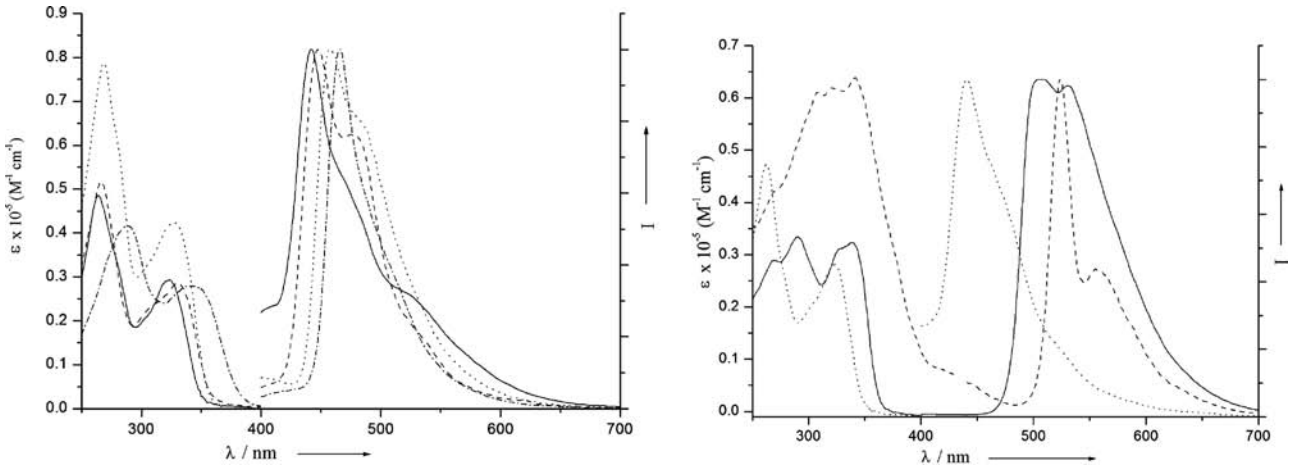

Figure 3. (Left) Electronic absorption spectra of **2** (—), **3** (----), **4** (· · · ·), and **5** (-·-·-·) and normalized emission spectra of **2** (—), **3** (----), **4** (· · · ·), and **5** (-·-·-) in degassed CH_2Cl_2 at 298 K. (Right) Electronic absorption spectra of **6** (—), **7** (----), and **9** (· · · ·) and normalized emission spectra of **6** (—), **7** (----), and **9** (· · · ·), in degassed CH_2Cl_2 at 298 K.

Table 1. Photophysical Properties of Complexes **2**−**9**

	room temperature solution (CH_2Cl_2)						77 K glass[b]
complex	absorption λ_{max}[nm] (ε_{max}/[dm^3 mol^{-1}cm^{-1}])	emission λ_{max} [nm]	τ [ns]	Φ_{em}[a]	k_r [s^{-1}] × 10^3	K_{nr} [s^{-1}] × 10^5	(2-MeTHF)
2	264(48600), 324(29400)	442, 482 sh	27.1	2.4×10^{-3}	88.6	368.1	437, 456 sh
3	266(51700), 330(28600)	447, 475 sh	44.0	1.8×10^{-3}	40.9	226.9	440, 484 sh
4	269(78700), 327(42500)	458, 482 sh	963.7	4.8×10^{-3}	5.0	10.3	444, 478 sh
5	288(41600), 341(27900)	465	844.1	3.4×10^{-2}	40.3	11.4	454, 481 sh
6	290(33400), 340(32400)	506, 530 sh	6335.1	1.1×10^{-2}	1.7	1.6	493, 508 sh
7	341(63800)	524, 555 sh	28982.0	1.9×10^{-2}	0.7	0.3	520, 553 sh
8	290(67400), 369(66500), 399(64700)	664, 725 sh	*c*	1.8×10^{-3}			659, 677 sh
9	263(47200), 323(28100)	440, 475 sh	27.2	8.2×10^{-3}	301.5	364.6	429, 455 sh

[a] Photoluminescence quantum yield determined with quinine sulfate as standard at 298 K. [b] Vibronic structured emission bands. [c] Multiexponential decay.

with increasing σ-donicity and greater conjugation, are consistent with a mainly metal-based HOMO and a π^* acetylide LUMO. All the Pt(II) complexes **2**−**9** displayed moderate phosphorescence intensity with quantum yields of emission between 1.8×10^{-3} and 3.4×10^{-2} in RT deoxygenated fluid solution and exhibited weak solvatochromic behavior (see Figure S2 in the Supporting Information). At 77 K, a rigidochromic shift of 4−14 nm was observed (see Figure S4 in the Supporting Information). The rigid glass does not allow the reorganization of the solvent dipoles upon generation of excited states and gives strongly blue-shifted spectra of complexes that emit from charge-transfer states. The above observed trend along with the vibronically structured nature of emission at 77 K suggests that the origin of emission occurs from admixed MLCT and interligand $\pi-\pi^*$ states. Stokes shifts of the lower lying emission in the range of 115−265 nm and lifetimes in the nanosecond to sub-microsecond regime, together with the observation of a 5- to 10-fold decrease in PL intensities upon exposure to molecular dioxygen, further support the phosphorescent nature of the emission.

Table 2. Electrochemical Data for Complexes **1**−**9**[a]

complex	E_{ox} (V)
1	+0.28
2	+0.58
3	+0.47
4	+0.46
5	−0.05
6	+0.50
7	+0.67
8	+0.33
9	+0.60

[a] Scan rate = 100 mV s^{-1} in 0.1 M [nBu$_4$][PF$_6$] (Au elelctrode; E vs $Fc^{0/+}$; 20 °C; CH_2Cl_2).

The cyclic voltammograms of all complexes showed similar redox profiles. In DCM/0.1 M TBAP, all complexes show an irreversible oxidation wave between +0.67 and −0.05 V (Table 2). A qualitative relationship between the oxidation potential of the alkynes and their respective emission energy was observed. In general, the oxidation potential was in decreasing order (**9** > **2** > **3** > **4** > **5**) with the increasing electron richness of the arylacetylide

(38) Frisch, M. J.; Trucks, G. W.; Schlegel, H. B.; Scuseria, G. E.; Rob, M. A.; Cheeseman, J. R.; Montgomery, J. A., Jr.; Vreven, T.; Kudin, K. N.; Burant, J. C.; Millam, J. M.; Iyengar, S. S.; Tomasi, J.; Barone, V.; Mennucci, B.; Cossi, M.; Scalmani, G.; Rega, N.; Petersson, G. A.; Nakatsuji, H.; Hada, M.; Ehara, M.; Toyota, K.; Fukuda, R.; Hasegawa, J.; Ishida, M.; Nakajima, T.; Honda, Y.; Kitao, O.; Nakai, H.; Klene, M.; Li, X.; Knox, J. E.; Hratchian, H. P.; Cross, J. B.; Bakken, V.; Adamo, C.; Jaramillo, J.; Gomperts, R.; Stratmann, R. E.; Yazyev, O.; Austin, A. J.; Cammi, R.; Pomelli, C.; Ochterski, J. W.; Ayala, P. Y.; Morokuma, K.; Voth, G. A.; Salvador, P.; Dannenberg, J. J.; Zakrzewski, V. G.; Dapprich, S.; Daniels, A. D.; Strain, M. C.; Farkas, O.; Malick, D. K.; Rabuck, A. D.; Raghavachari, K.; Foresman, J. B.; Ortiz, J. V.; Cui, Q.; Baboul, A. G.; Clifford, S.; Cioslowski, J.; Stefanov, B. B.; Liu, G.; Liashenko, A.; Piskorz, P.; Komaromi, I.; Martin, R. L.; Fox, D. J.; Keith, T.; Al-Laham, M. A.; Peng, C. Y.; Nanayakkara, A.; Challacombe, M.; Gill, P. M. W.; Johnson, B.; Chen, W.; Wong, M. W.; Gonzalez, C.; Pople, J. A. *Gaussian 03*, Gaussian, Inc.: Wallingford, CT, 2003.

Table 3. Comparison between Selected DFT Optimized and X-Ray Bond Distances (Å) and Angles (deg)

	compd	symm	Pt−C_{carb}	Pt−C_{alk}	$(-C\equiv C-)_n$	≡C−R	C_{carb}−Pt−C_{carb}	C_{alk}−Pt−C_{alk}
1	X-ray	C_1	1.984(4)				83.91(16)	
			1.977(4)					
	DFT	Cs	1.974				85.6	
2	DFT	Cs	2.028	1.985	1.228	1.425	85.9	88.4
3	DFT	Cs	2.027	1.986	1.228	1.425	86.0	88.2
5	X-ray	C_1	2.001(11)	1.993(11)	1.194(14)	1.451(16)	83.4(5)	88.8(4)
			2.020(10)	1.990(9)	1.205(14)	1.460(15)		
	DFT	C_s	2.026	1.986	1.228	1.424	86.0	88.4
6	DFT	C_s	2.028	1.981	1.229	1.407	85.9	89.0
7	X-ray	C_s	2.026(11)	1.999(11)	1.209(15) (n = 1)	1.440(16)	85.4(6)	88.6(6)
					1.203(17) (n = 2)			
	DFT	C_s	2.028	1.984	1.228 (n = 1)	1.421	85.9	88.7
					1.218 (n = 2)			
8	DFT	C_1	2.028	1.983	1.229	1.420	86.0	87.8
			2.029	1.983	1.229	1.420		
9	DFT	Cs	2.028	1.986	1.228	1.425	85.9	88.2

Table 4. Selected Singlet−Singlet (S_n) and Singlet−Triplet (T_1) Excited States with TDDFT/CPCM Vertical Excitation Energies (nm), Transition Coefficients, Orbitals Involved in the Transitions, and Oscillator Strengths for Compounds **2**−**9**

	2	**3**	**5**	**6**	**7**	**8**	**9**
				absorption			
exp λ_{abs}	264, 324	266, 330	288, 341	290, 340	341	290, 369, 399	262, 323
calc λ_{abs} [a]	289, 329	281, 344	286, 370	291, 354	372	410	277, 330
S_0-S_n	n = 1	n = 1	n = 1	n = 1	n = 1	n = 1	n = 1
	337 (0.481)	350 (0.496)	378 (0.534)	363 (0.561)	356 (1.565)	428 (0.833)	336 (0.458)
	H→L (0.68)	H→L (0.68)	H→L (0.68)	H→L (0.68)	H→L (0.65)	H→L (0.65)	H→L (0.68)
S_0-S_n	n = 2	n = 2	n = 2	n = 2	n = 2	n = 2	n = 2
	335 (0.376)	343 (0.434)	363 (0.563)	346 (0.478)	372 (1.258)	408 (0.533	334 (0.392)
	H-1→L (0.67)	H-1→L (0.68)	H-1→L (0.68)	H-1→L (0.67)	H-1→L (0.65)	H-1→L (0.66)	H-1→L (0.67)
S_0-S_n	n = 3	n = 3	n = 7	n = 5	n = 3	n = 3	n = 3
	304 (0.172)	302 (0.118)	290 (0.182)	290 (0.218)	342 (0.655)	389 (0.363)	302 (0.151)
	H-2→L (0.67)	H-2→L (0.68)	H→L+4 (0.53)	H→L+1 (0.59)	H→L+1 (0.65)	H→L+1 (0.66)	H-2→L (0.67)
S_0-S_n	n = 5	n = 5	n = 8	n = 6	n = 4	n = 4	n = 7
	282 (0.055)	286 (0.066)	284 (0.577)	287 (0.239)	340 (0.346)	382 (0.200)	275 (0.060)
	H-4→L (0.66)	H→L+2 (0.53)	H→L+1 (0.58)	H-1→L+1 (0.61)	H-1→L+1 (0.65)	H-1→L+1 (0.67)	H-4→L (0.66)
S_0-S_n	n = 6	n = 8	n = 9	n = 7	n = 10	n = 10	n = 8
	282 (0.358)	280 (0.409)	282 (0.352)	282 (0.049)	285 (0.067)	321 (0.090)	274 (0.312)
	H-1→L+1 (0.62)	H-1→L+1 (0.47)	H→L+5 (0.43)	H-4→L (0.65)	H-3→L+1 (0.53)	H-1→L+2 (0.52)	H→L+1 (0.65)
S_0-S_n	n = 7	n = 9	n = 10				n = 11
	279 (0.280)	278 (0.446)	282 (0.069)				273 (0.352)
	H→L+1 (0.65)	H-2→L+1 (0.43)	H-1→L+4 (0.51)				H-1→L+1 (0.57)
				Emission			
exp λ_{emiss}	442	447	465	506	524	664	440
calc λ_{emiss} [b]	454	461	485	546	562	683	453
S_0-T_1	437	442	464	504	549	698	436
	H→L (0.57)	H→L (0.58)	H→L (0.60)	H→L (0.61)	H→L (0.57)	H→L (0.53)	H→L (0.57)

[a] The calculated values are obtained from the TDDFT/CPCM UV−vis spectra drawn by Gaussview. [b] Solvent-corrected energy difference between the optimized ground state and the lowest-lying triplet state.

ancillary ligands. The correlation exemplifies the similarity between the electrochemical and spectroscopic trend. However, it should be noted here that complexes **6**−**8** did not obey the above tendency. Oxidation of the [(pmim)Pt-(C≡C−R)$_2$] was not observed in most cases up to +1.5 V. This result is comparable to the behavior observed in Pt(diimine)(C≡C−R)$_2$ complexes.

DFT and TD-DFT Calculations. In order to support the photophysical assignments from experimental observations, TD-DFT and DFT calculations were carried out for most of the studied complexes (**1** - **3** and **5** − **9**). All calculations were performed with the Gaussian03 program package[38] using the hybrid functional PBE1PBE[39] in conjunction with the Stuttgart/Dresden effective core potentials (SDD) basis set[40] for the Pt center augmented with one f-polarization function (exponent α = 0.993) and the standard 6-31+G(d) basis set[41] for the remaining atoms. For computational ease, the *n*-pentyl chain was replaced by a methyl group and the details about the DFT-optimized geometries are presented in Supporting Information. The main geometric parameters of the calculated complexes, especially the bond distances and angles around the Pt metal center and the C≡C triple bond distances, obtained with the combination PBE1PBE/SDD:6-31+g(d) were in a good agreement with those from the X-ray structures (Table 3).

(39) Adamo, C.; Barone, V. *J. Chem. Phys.* **1999**, *110*, 6158–6170.

(40) Dunning, T. H., Jr.; Hay, P. J. *Modern Theoretical Chemistry*; Plenum: New York, 1976; Vol. *3*.

(41) Ditchfie, R.; Hehre, W. J.; Pople, J. A. *J. Chem. Phys.* **1971**, *54*, 724.

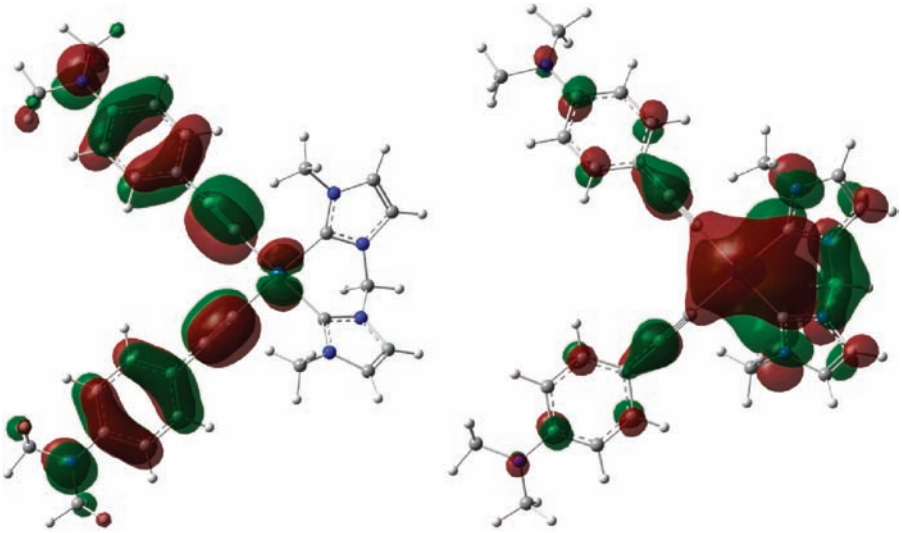

Figure 4. HOMO (left) and LUMO (right) of **5**.

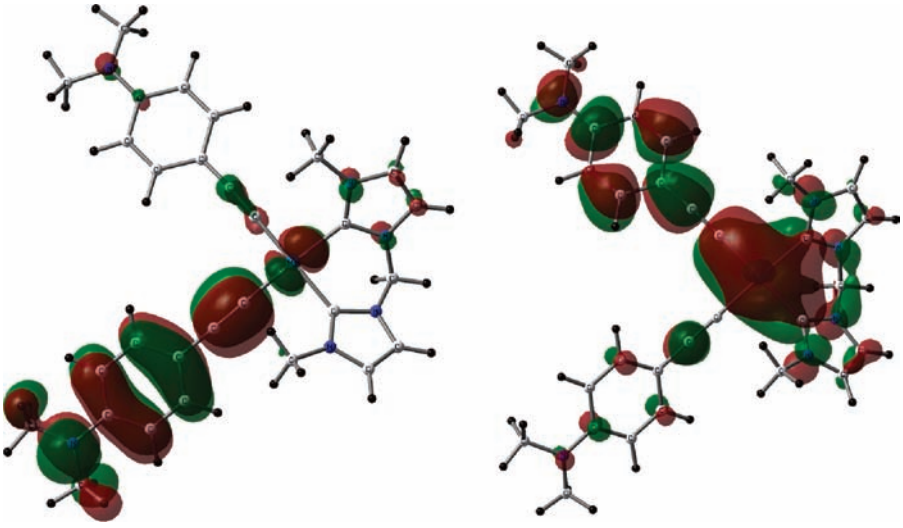

Figure 5. Lower- (left) and higher-energy SOMO (right) of the triplet excited state of **5**.

The main geometric parameters of the calculated complexes, especially the bond distances and angles around the Pt metal center and the C≡C triple bond distances, obtained with the combination PBE1PBE/SDD:6-31+g(d) are in a good agreement with those from the X-ray structures (Table 3). The calculated UV−vis spectra of the studied compounds also mimic the experimental results very well with two sharp and distinct absorption bands in the region of 250−450 nm for **2** and **3**, **5** and **6**, and **8** and **9**, and only one band for **7** in the same UV−visible region (Table 4). Although the vertical singlet−triplet transitions ($S_0 \rightarrow T_1$) calculated on the ground state geometries were very satisfactory for estimating the emission maxima of the studied compounds since $\Delta\lambda_{max}$ is for five complexes as low as 2−5 nm (overall $2 < \Delta\lambda_{max} < 33$ nm, Table 3), we thought that emission maxima calculated from the energy differences between the ground- and triplet-excited states would be more relevant theoretically. For this purpose, solvent effects (dichloromethane) were included by single-point calculations on the optimized gas-phase geometries. The corresponding solvent-corrected energy differences calculated for the studied compounds are reported in Table 3 as calc λ_{emiss}. Surprinsigly, these new values exhibit a larger overestimation of the emission maxima ($13 < \Delta\lambda < 42$ nm, Table 3); however, the tendency is still correct from one compound to another (Supporting Information).

It appeared from the TD-DFT calculations that the HOMO−LUMO gap and consequently the shape of these frontier orbitals play a major role in the absorption and emission properties of our complexes. Taking **5** as an exemplary molecule, the most red band of the absorption spectrum corresponds to H → L and H-1 → L; the HOMO is of π character mainly based on the C≡C−R π orbitals (93%) in an out-of-phase combination with the Pt $5d_{xy}$ orbital (6%). The participation of the *N*-heterocyclic dicarbene in the HOMO is very weak (1%). The LUMO is clearly delocalized over the whole molecule with 32% on the alkyne ligands, 35% on the dicarbene ligand, and 33% on the empty Pt $6p_y$ metal (Figure 4). The shape of the LUMO exhibits a bonding interaction between the p_y atomic orbitals of the Pt and C_{alk} atoms and an antibonding interaction between the p_y atomic orbitals of the triply bonded C atoms of the alkyne ligands. Consequently,

the red-shifted band of the UV−vis spectrum can be assigned to an admixture of metal-perturbed intraligand ^{1}ILCT ($\pi_{alk} \rightarrow \pi^*_{alk}$), metal-perturbed ligand-to-ligand ^{1}LLCT ($\pi_{alk} \rightarrow \pi^*_{carb}$), and metal-to-ligand ^{1}MLCT transitions. The blue-shifted band appears to get its origins from different occupied frontier orbitals and the only LUMO+1. Since H and L+1 are both composed at 93 and 88% of π orbitals of the alkyne atoms (only 6 and 4% of Pt), the absorption band can easily be assigned as a metal-perturbed intraligand ^{1}ILCT ($\pi_{alk} \rightarrow \pi^*_{alk}$).

The transition responsible for the emission band of **5** involves the migration of one electron from the HOMO to the LUMO, leading to the two singly occupied molecular orbitals (SOMOs) of the triplet excited state. Both SOMOs have contributions mainly from only one of the alkyne ligands (also with participation of the carbene and the metal center): the lower-energy SOMO is localized on one alkyne, and the higher-energy SOMO involves the other one (Figure 5). The modifications of the geometrical parameters of the optimized triplet state relative to the ground state structure confirm this observation. Indeed, the main changes occur for only one alkyne ligand in which the Pt−C and the C−C_{ring} are shortened and the C≡C bond is elongated, a consequence of the π-bonding and π-antibonding interactions seen in the higher-energy SOMO (Figure 5) derived from the former LUMO of the ground state. The unchanged alkyne is the one which does not participate in the higher-energy SOMO. This provides a clear indication that the triplet excited state of **5** contains mainly the metal-perturbed ligand-to-ligand ^{3}LLCT ($\pi_{alk} \rightarrow \pi^*_{alk}$) character and to a lesser extent the ^{3}MLCT (d $\rightarrow \pi^*_{alk}$). Since the calculations revealed a similar behavior for all compounds, we can extend this conclusion to all of them.

Conclusions

A series of luminescent platinum(II) alkynyl complexes of the type [(pmim)Pt(C≡C−R)$_2$] (R = C_6H_5, C_6H_4OMe, $C_6H_2(OMe)_3$, $C_6H_4NMe_2$, C_4H_3S, $C_6H_4C{\equiv}CC_6H_5$, 1-pyrenyl, and C_6H_4F) were successfully synthesized starting from the corresponding diiodide complex [(pmim)PtI$_2$]. These complexes are found to be emissive at room temperature with their lowest lying emissive states tunable and assigned from predominantly metal-perturbed ligand-to-ligand ^{3}LLCT ($\pi_{alk} \rightarrow \pi^*_{alk}$) character and to a lesser extent the ^{3}MLCT (d $\rightarrow \pi^*_{alk}$). Through further rational design and synthetic methodologies, these new alkynyl complexes can be utilized for the buildup of luminescent functional materials.

Experimental Section

General Procedure. All manipulations requiring an inert atmosphere were carried out using standard Schlenk techniques under dinitrogen. ^{1}H, ^{13}C{^{1}H}, and ^{19}F NMR spectra were recorded on Bruker AV2-300 (300 MHz) or AV-500 (500 MHz) spectrometers. Chemical shifts (δ) are reported in parts per million (ppm) referenced to tetramethylsilane (δ 0.00) ppm using the residual protio solvent peaks as internal standards (^{1}H NMR experiments) or the characteristic resonances of the solvent nuclei (^{13}C NMR experiments). ^{19}F NMR was referenced to $CFCl_3$ (δ 0.00) ppm. Coupling constants (J) are quoted in Hertz (Hz), and the following abbreviations are used to describe the signal multiplicities: s (singlet), d (doublet), t (triplet), q (quartet), m (multiplet), and dm (doublet of multiplet). Proton and carbon assignments have been made using routine one- and two-dimensional NMR spectroscopies where appropriate. Infrared (IR) spectra were recorded on a Perkin-Elmer 1600 Fourier Transform spectrophotometer using KBr pellets with frequencies (ν_{max}) quoted in wavenumbers (cm^{-1}). Elemental microanalysis was carried out with a Leco CHNS-932 analyzer. Mass spectra were run on a Finnigan-MAT-8400 mass spectrometer. TLC analysis was performed on precoated Merck Silica Gel 60F_{254} slides and visualized by luminescence quenching either at (short wavelength) 254 nm or (long wavelength) 365 nm. Chromatographic purification of products was performed on a short column (length 15.0 cm, diameter 1.5 cm) using silica gel 60 and 230−400 mesh using a forced flow of eluent. UV−vis measurements were carried out on a Perkin-Elmer Lambda 19 UV/vis spectrophotometer. Emission spectra were acquired on a Perkin-Elmer spectrophotometer using 450 W xenon lamp excitation by exciting at the longest-wavelength absorption maxima. All samples for emission spectra were degassed by at least three freeze−pump−thaw cycles in an anaerobic cuvette and were pressurized with N_2 following each cycle. The 77 K emission spectra were acquired in frozen 2-methyltetrahydrofuran (2-MeTHF) glass. Luminescence quantum yields of ϕ were determined at 298 K (estimated uncertainty ±15%) using standard methods; wavelength-integrated intensities (I) of the corrected emission spectra were compared to iso-absorptive spectra of the quinine sulfate standard (ϕ_r = 0.54 in 1N H_2SO_4 air-equilibrated solution) and were corrected for the solvent refractive index. Phosphorescence lifetime measurements were performed on an Edinburgh FLS920 spectrophotometer, using nF900 with a 30 000 Hz frequency, with 15 nm excitation and 15 nm emission slit widths.

All starting materials were purchased from commercial sources and used as received unless stated otherwise. The solvents used for synthesis were of analytical grade. The compounds 4-methoxyphenylacetylene, 2-ethynylthiophene, 2,3,4-trimethoxyphenylacetylene, and 4-(phenylethynyl)phenylacetylene were prepared according to literature methods.

[Pt(pmim)$_2$I$_2$] (1). Platinum(II) acetylacetonate (Pt(acac)$_2$) (0.197 g, 0.5 mmol) was dissolved in DMSO (3 mL) and heated to 100 °C. The ligand pmim (0.272 g, 0.5 mmol) dissolved in DMSO (20 mL) was slowly added to the hot solution of Pt(acac)$_2$ for a period of 10 h. The reaction mixture was then stirred at 100 °C for another 2 h, and the DMSO was removed *in vacuo*. The resulting product was purified by column chromatography over silica gel with the acetone/*n*-hexane (v/v 4:5) as the eluent. The pure compound was isolated as a white powder. Crystals suitable for X-ray were obtained from a mixture of dichloromethane and pentane. (Crystallographic data for compounds **1**, **4**, **5**, and **7** are giving in Table 5.) Yield: 62%. ^{1}H NMR (500 MHz, CD_2Cl_2, 20 °C): δ (ppm) 7.31 (d, 2H, ^3J = 2.5 Hz, NC*H*=CHN), 6.91 (d, 2H, ^3J = 2.0 Hz, NCH=C*H*N), 6.23 (d, H, ^2J = 13.0 Hz, NCH_2N), 5.80 (d, H, ^2J = 13.0 Hz, NCH_2N), 4.73 (m, 2H, NCH_2CH$_2$), 4.08 (m, 2H, NCH_2CH$_2$), 1.84 (m, 4H, NCH$_2$CH_2CH$_2$), 1.27 (m, 8H, CH$_2$CH_2CH_2CH$_3$), 0.86 (t, 6H, ^3J = 2.0 Hz, CH$_2$CH_3). ^{13}C{^{1}H} NMR (125.8 MHz, CD_2Cl_2, 20 °C), δ (ppm) = 151.3 ($J_{Pt=C}$ = 1373 Hz), 121.1 and 120.3 (N*C*H=*C*HN), 63.6 (N*C*H$_2$N), 52.3, 31.0, 28.6, 22.5, 14.0 (C on the (CH$_2$)$_4$CH$_3$). ESI$^+$ MS m/z: 687.5 (M$^+$). Elemental analysis calcd for $C_{17}H_{30}I_2N_4Pt$: C, 27.60; H, 4.09; N, 7.58. Found: C, 27.81; H, 4.03; N, 7.58.

General Procedure for the Synthesis of Complexes 2−9. All manipulations were performed under a N_2 atmosphere. Two equivalents of *n*-BuLi were added to the flask containing 2 equiv of the ligand in THF (10 mL) at −78 °C, and the reaction mixture was stirred for 30 min at this temperature. The temperature was then gradually raised to room temperature and stirred for another 30 min. The reaction mixture was then transferred to a flask containing starting material (**1**) dissolved in THF (10 mL) at −78 °C and stirred for 30 min at this temperature. The

Table 5. Crystallographic Data for Compounds **1**, **4**, **5**, and **7**[a]

	1	**4**	**5**	**7**
empirical formula	$2(C_{17}H_{28}I_2N_4Pt)$, $5(CH_2Cl_2)$	$C_{39}H_{50}N_4O_6Pt$, CH_2Cl_2	$2(C_{37}H_{48}N_6Pt)$, $3(CH_2Cl_2)$	$C_{49}H_{46}N_4Pt$, CH_2Cl_2
fw (g mol^{-1})	1899.26	950.84	1798.57	970.90
temp (K)	183(2)	183(2)	183(2)	183(2)
wavelength (Å)	0.71073	0.71073	0.71073	0.71073
cryst syst, space group	monoclinic, *C*2/*c*	monoclinic, $P2_1/n$	monoclinic, *C*2/*c*	orthorhombic, *Pnma*
a (Å)	31.7153(11)	14.7205(2)	25.9714(6)	10.2966(3)
b (Å)	9.0519(3)	20.6676(2)	10.0221(2)	36.5438(9)
c (Å)	21.9061(18)	15.2338(2)	31.4262(7)	11.4905(2)
α (deg)	90	90	90	90
β (deg)	102.644(5)	117.138(1)	90.715(2)	90
γ (deg)	90	90	90	90
volume (Å^3)	6136.4(6)	4124.46(9)	8179.2(3)	4323.61(18)
Z, density (calcd) (Mg m^{-3})	4, 2.056	4, 1.531	4, 1.461	4, 1.492
abs coefficient (mm^{-1})	7.037	3.581	3.661	3.408
F(000)	3576	1920	3624	1952
cryst size (mm^3)	0.48 × 0.33 × 0.07	0.32 × 0.11 × 0.05	0.17 × 0.07 × 0.03	0.16 × 0.11 × 0.03
θ range (deg)	2.6 to 30.5	2.5 to 30.5	2.5 to 25.0	2.7 to 25.7
reflns collected	27259	59674	32595	19026
reflns unique	9355/R_{int} = 0.0355	12584/R_{int} = 0.0417	7199/R_{int} = 0.0852	4048/R_{int} = 0.0568
completeness to *θ* (%)	99.9	99.9	99.9	97.0
absorption correction	analytical	analytical	analytical	analytical
max/min transmission	0.632 and 0.128	0.839 and 0.583	0.912 and 0.661	0.906 and 0.672
data/restraints/params	6910/62/308	9450/15/486	5024/53/443	3136/0/272
goodness-of-fit on F^2	0.983	0.915	1.109	1.180
final R_1 and wR_2 indices [$I > 2\sigma(I)$]	0.0344, 0.0713	0.0253, 0.0531	0.0764, 0.1272	0.0699, 0.1625
R_1 and wR_2 indices (all data)	0.0571, 0.0752	0.0396, 0.0545	0.1327, 0.1417	0.0887, 0.1670

[a] The unweighted *R* factor is $R_1 = \sum(F_o - F_c)/\sum F_o$, $I > 2\,\sigma(I)$, and the weighted *R* factor is $wR_2 = \{\sum w(F_o^2 - F_c^2)^2/\sum w(F_o^2)^2\}^{1/2}$.

temperature was gradually raised to room temperature and stirred for another 1 h. After H_2O (10 mL) was added, the product was extracted with CH_2Cl_2 (3 × 10 mL). The organic layer was separated and dried over $MgSO_4$. The solvent was evaporated to dryness, and the compound was purified by column chromatography over silica gel.

[Pt(pmim)$_2$(C≡C−C$_6$H$_5$)$_2$] (2). EtOAc/CH_2Cl_2 (3:7 v/v) was used as the eluent. Yield: 52%. ^{1}H NMR (500 MHz, CD_2Cl_2, 20 °C): *δ* (ppm) 7.28 (d, 2H, ^3J = 1.5 Hz, NC*H*=CHN), 7.24 (d, 4H, ^3J = 10.0 Hz, *o*-Phenyl H), 7.16 (t, 4H, ^3J = 6.0 Hz, *m*-Phenyl H), 7.06 (t, 2H, ^3J = 6.5 Hz, *p*-Phenyl H), 6.79 (d, ^3J = 1.5 Hz, NCH=C*H*N), 5.95 (s, 2H, NCH_2N), 4.96 (m, 2H, NCH_2CH$_2$), 4.18 (m, 2H, NCH_2CH$_2$), 1.76 (m, 4H, NCH$_2$-CH_2CH$_2$), 1.21 (m, 8H, CH$_2$CH_2CH_2CH$_3$), 0.78 (t, 6H, ^3J = 7.5 Hz, CH$_2$CH_3). ^{13}C{^{1}H} NMR (125.8 MHz, CD_2Cl_2, 20 °C): *δ* (ppm) 167.8 (*C*=Pt), 131.1, 128.1, 124.9 (C on Phenyl ring), 129.1 (C≡*C*−Pt), 120.3 and 120.2 (N*C*H=*C*HN), 108.9 and 106.8 (Ph*C*≡*C*−Pt), 63.2 (N*C*H$_2$N), 50.8, 31.3, 28.9, 22.6, 13.9 (C on the (CH$_2$)$_4$CH$_3$). ESI$^+$ MS *m*/*z*: 687.5 (M$^+$). IR (ATR, cm^{-1}) $\nu_{C\equiv C}$ = 2098. Elemental analysis calcd for $C_{33}H_{40}N_4Pt$: C, 57.63; H, 5.86; N, 8.15. Found: C, 57.79; H, 5.89; N, 8.20.

[Pt(pmim)$_2$(C≡C−C$_6$H$_4$−OCH$_3$)$_2$] (3). EtOAc/CH_2Cl_2 (2:8 v/v) was used as the eluent. Yield: 74%. ^{1}H NMR (500 MHz, CD_2Cl_2, 20 °C): *δ* (ppm) = 7.23 (d, 4H, ^3J = 10.0 Hz, *o*-Phenyl H), 7.15 (d, 2H, ^3J = 2.0 Hz, *H*C=CH), 6.88 (d, 2H, ^3J = 2.0 Hz, HC=C*H*), 6.73 (d, 4H, ^3J = 10.0 Hz, m-Phenyl H), 6.09 (d, 1H, ^2J = 12.5 Hz, NCH_2N), 5.62 (d, 1H, ^2J = 13.0 Hz, NCH_2N), 4.98 (m, 2H, NCH_2CH$_2$), 4.24 (m, 2H, NCH_2CH$_2$), 3.74 (s, 6H, OCH_3), 1.81 (m, 4H, NCH$_2$CH_2CH$_2$), 1.21 (m, 8H, CH$_2$CH_2CH_2CH$_3$), 0.78 (t, 6H, ^3J = 7.0 Hz, CH$_2$CH_3). ^{13}C-{^{1}H} NMR (125.8 MHz, CD_2Cl_2, 20 °C), *δ* (ppm) 168.4 (C=Pt), 157.3, 132.3, 121.7, and 113.5 (C on Phenyl ring), 120.7 and 119.7 (N*C*=*C*N), 108.1 and 103.5 (Ph*C*=*C*−Pt), 63.5 (N*C*H$_2$N), 55.4 (O−*C*H$_3$), 50.9, 31.3, 29.0, 22.6, 14.0 (C on the (CH$_2$)$_4$CH$_3$). ESI$^+$ MS *m*/*z*: 746.4 (M$^+$). IR (ATR, cm^{-1}) $\nu_{C\equiv C}$ = 2107. Elemental analysis calcd (%) for $C_{35}H_{44}N_4O_2Pt$: C, 56.21; H, 5.94; N, 7.49. Found: C, 56.38; H, 6.01; N, 7.34.

[Pt(pmim)$_2$(C≡C−C$_6$H$_2$(OCH$_3$)$_3$)$_2$] (4). EtOAc was used as the eluent. Yield: 84%. ^{1}H NMR (500 MHz, CD_2Cl_2, 20 °C): *δ* (ppm) 7.18 (d, 2H, ^3J = 1.5 Hz, *H*C=CH), 6.89 (d, 2H, ^3J = 2.0 Hz, HC=C*H*), 6.55 (s, 4H, *o*-Phenyl H), 6.09 (d, 1H, ^2J = 12.5 Hz, NCH_2N), 5.69 (d, 1H, ^2J = 11.5 Hz, NCH_2N), 4.93 (m, 2H, NCH_2CH$_2$), 4.28 (m, 2H, NCH_2CH$_2$), 3.7 (m, 12H, OCH_3), 3.71(m, 6H, OCH_3), 1.79 (m, 4H, NCH$_2$CH_2CH$_2$), 1.21 (m, 8H, CH$_2$CH_2CH_2CH$_3$), 0.77 (t, 6H, ^3J = 7.0 Hz, CH$_2$CH_3). ^{13}C-{^{1}H} NMR (125.8 MHz, CD_2Cl_2, 20 °C): *δ* (ppm) 171.7 (*C*=Pt), 153.0, 136.4, 124.5, 108.3, and 105.5 (C on the phenyl ring), 120.7 and 119.7 (N*C*=*C*N), 110.1 (*C*-Pt), 63.5 (N*C*H$_2$N), 60.7 and 56.1 (O-*C*H$_3$), 51.0, 33.6, 31.4, 23.7, 14.0 (C on the (CH$_2$)$_4$CH$_3$). ESI$^+$ MS *m*/*z*: 866.5 (M$^+$). IR(ATR, cm^{-1}) $\nu_{C\equiv C}$ = 2096. Elemental analysis calcd for $C_{39}H_{52}N_4O_6Pt$: C, 53.97; H, 6.04; N, 6.46. Found: C, 53.74; H, 6.10; N, 6.54.

[Pt(pmim)$_2$(C≡C−C$_6$H$_4$−N(CH$_3$)$_2$)$_2$] (5). EtOAc/CH_2Cl_2 (1:9 v/v) was used as the eluent. Single crystals suitable for X-ray diffraction studies were obtained from a mixture of dichloromethane and pentane. Yield: 43%. ^{1}H NMR (500 MHz, CD_2Cl_2, 20 °C): *δ* (ppm) 7.19 (d, 4H, ^3J = 9.0 Hz, *o*-Phenyl H), 7.09 (d, 2H, ^3J = 2.0 Hz, NC*H*CHN), 6.90 (d, 2H, ^3J = 1.5 Hz, NC*H*CHN), 6.60 (d, 4H, ^2J = 4.5 Hz, *m*-phenyl H), 6.13 (d, 1H, ^2J = 12.5 Hz, NCH_2N), 5.52 (d, H, ^2J = 12.5 Hz, NCH_2N), 5.13 (m, 2H, NCH_2CH$_2$), 4.17 (m, 2H, NCH_2CH$_2$), 2.89 (s 12H, N(CH$_3$)$_2$), 1.80 (m, 4H, CH$_2$CH_2CH$_2$), 1.23 (m, 8H, CH$_2$CH_2CH_2CH$_3$), 0.80 (t, 6H, ^3J = 7.0 Hz, CH$_2$CH_3). ^{13}C{^{1}H} NMR (125.8 MHz, CD_2Cl_2, 20 °C): *δ* 169.0 (*C*=Pt), 148.5, 132.2, 117.7, and 112.5 (C on the phenyl ring), 120.6 and 119.4 (N*C*=*C*N), 108.9 and 102.0 (Ph*C*=*C*−Pt), 63.6 (N*C*H$_2$N), 40.7 (C on the N(*C*H$_3$)$_2$), 50.9, 31.4, 29.0, 22.7, 14.0 (C on the (CH$_2$)$_4$CH$_3$). ESI$^+$ MS *m*/*z*: 772.5 (M$^+$). IR (ATR, cm^{-1}) $\nu_{C\equiv C}$ = 2098. Elemental analysis calcd for $C_{37}H_{50}N_6Pt$: C, 57.42; H, 6.51; N, 10.86. Found: C, 57.69; H, 6.40; N, 10.63.

[Pt(pmim)$_2$(C≡C−Ph−C≡C−Ph)$_2$] (6). EtOAc/CH_2Cl_2 (1:9 v/v) was used as the eluent. Single crystals suitable for X-ray diffraction studies were obtained from a mixture of dichloromethane and diethyl ether. Yield: 36%. ^{1}H NMR (500 MHz, CD_2Cl_2, 20 °C): *δ* (ppm) 7.51 (m, 4H, Phenyl H), 7.34 (m, 10H, phenyl H), 7.26 (m, 4H, phenyl H), 7.24 (d, 2H, ^3J = 2.0 Hz, NCHC*H*N), 6.86 (d, ^3J = 2.0 Hz, NCHC*H*N), 6.06 (d, 2H, ^2J = 13.0 Hz, NCH_2N), 5.84 (d, 2H, ^2J = 13.0 Hz, NCH_2N), 4.90 (m, 2H, NCH_2CH$_2$), 4.24 (m, 2H, NCH_2CH$_2$), 1.81 (m, 4H, NCH$_2$CH_2CH$_2$), 1.23 (m, 8H, CH$_2$CH_2CH_2CH$_3$), 0.79 (t, 6H,

^3J = 7.0 Hz, CH_2CH_3). $^{13}C\{^1H\}$ NMR (125.8 MHz, CD_2Cl_2, 20 °C): δ (ppm) 167.6 (*C*═Pt), 131.6, 131.3, 131.2, 129.3, 128.6, 128.3, 123.7, and 119.2 (C on the phenyl ring), 120.6 and 120.0 (N*C*═*C*N), 110.4 (C≡*C*−Pt), 109.1 (*C*≡C−Pt), 90.1 and 89.8 (Ph*C*≡*C*Ph), 63.4 (N*C*H_2N), 50.9, 31.3, 29.0, 22.6, and 14.0 (C on the $(CH_2)_4CH_3$). ESI^+ MS *m*/*z*: 886.5 (M^+). IR (ATR, cm^{-1}) $\nu_{C\equiv C}$ = 2094. Elemental analysis calcd for $C_{49}H_{48}N_4Pt$: C, 66.27; H, 5.45; N, 6.31. Found: C, 65.95; H, 5.66; N, 6.16.

[Pt(pmim)$_2$(C≡C−2-thienyl)$_2$] (7). EtOAc/CH_2Cl_2 (1:9 v/v) was used as the eluent. Yield: 55%. ^1H NMR (500 MHz, CD_2Cl_2, 20 °C): δ (ppm) 7.28 (d, 2H, ^3J = 1.5 Hz, NC*H*CHN), 6.95 (d, 2H, ^3J = 1.5 Hz, NCHC*H*N), 6.84 (m, 6H, H on thienyl), 5.95 (d, H, ^2J = 13.0 Hz, NCH_2N), 5.88 (d, H, ^2J = 13.0 Hz, NCH_2N), 4.90 (m, 2H, NCH_2CH_2), 4.16 (m, 2H, NCH_2CH_2), 1.78 (m, 4H, $NCH_2CH_2CH_2$), 1.22 (m, 8H, $CH_2CH_2CH_2CH_3$), 0.86 (t, 6H, ^3J = 3.5, CH_2CH_3). $^{13}C\{^1H\}$ NMR (125.8 MHz, CD_2Cl_2, 20 °C): δ (ppm) 167.2 (*C*═Pt), 129.9, 127.6, 126.7, and 122.7 (C on thienyl ring), 120.5 (N*C*═CN), 120.2 (NC═*C*N), 111.9 (C≡*C*−Pt), 100.5 (*C*≡C−Pt), 63.4 (N*C*H_2N), 50.9, 31.3, 28.9, 22.6, 14.0 (C on the $(CH_2)_4CH_3$)). ESI^+ MS *m*/*z*: 698.3 (M^+). IR (ART, cm^{-1}) $\nu_{C\equiv C}$ = 2090. Elemental analysis calcd for $C_{29}H_{36}N_4S_2Pt$: C, 49.77; H, 5.18; N, 8.01. Found: C, 49.69; H, 5.25; N, 8.04.

[Pt(pmim)$_2$(C≡C-2-Pyrenyl)$_2$] (8). EtOAc/CH_2Cl_2 (1:3 v/v) was used as the eluent. Yield: 46%. ^1H NMR (500 MHz, CD_2Cl_2, 20 °C): δ 9.04 (d, 1H, ^3J = 10.0 Hz, H on the pyrenyl), 8.1, 8.0, 7.9, 7.8 (m, 8H, H on the pyrenyl), 7.18 (d, ^3J = 1.5 Hz, NCHC*H*N), 6.95 (d, ^3J = 1.5 Hz, NC*H*CHN), 6.29 (d, 1H, ^2J = 13.0 Hz, NCH_2N), 5.70 (d, 1H, ^2J = 13.0 Hz, NCH_2N), 5.18 (m, 2H, NCH_2CH_2), 4.40 (m, 2H, NCH_2CH_2), 1.90 (m, 4H, $NCH_2CH_2CH_2$), 1.21 (m, 8H, $CH_2CH_2CH_2CH_3$), 0.78 (t, 6H, ^3J = 7.5 Hz, CH_2CH_3). $^{13}C\{^1H\}$ NMR (125.8 MHz, CD_2Cl_2, 20 °C), δ (ppm) 168.3 (*C*═Pt), 131.9, 131.8, 131.7, 129.0, 125.0, and 125.0 (C on the pyrenyl ring without H), 129.5, 127.8, 127.8, 127.2, 126.5, 126.0, 124.8, 124.7, and 124.6 (C on the pyrenyl ring with H), 120.8 (N*C*═CN), 119.9 (NC═*C*N), 114.7 (C≡*C*−Pt), 108.0 (*C*≡C−Pt), 63.7 (N*C*H_2N), 51.3, 31.4, 28.9, 22.6, 13.9 (C on the $(CH_2)_4CH_3$)). ESI^+ MS *m*/*z*: 934.5 (M^+). IR (ATR,cm^{-1}) $\nu_{C\equiv C}$ = 2080. Elemental analysis calcd for $C_{53}H_{48}N_4Pt$: C, 68.01; H, 5.17; N, 5.99. Found: C, 67.91; H, 5.38; N, 5.83.

[Pt(pmim)$_2$(C≡C-4-C_6H_4F)$_2$] (9). EtOAc/CH_2Cl_2 (2:8 v/v) was used as an eluent. Yield: 76%. ^1H NMR (500 MHz, CD_2Cl_2, 20 °C): δ (ppm) 7.47 (d, 4H, ^3J = 8.0 Hz, Phenyl H), 7.09 (d, 2H, ^3J = 1.5 Hz, NC*H*═CHN), 6.92 (m, 4H, Phenyl H), 6.75 (d, 2H, ^3J = 1.5 Hz, NCH═C*H*N), 6.15 (d, 1H, ^2J = 13.0 Hz, NCH_2N), 5.67 (d, 1H, ^2J = 13.0 Hz, NCH_2N), 4.94 (m, 2H, NCH_2CH_2), 4.31 (m, 2H, NCH_2CH_2), 1.85 (m, 4H, $NCH_2CH_2CH_2$), 1.26 (m, 8H, $CH_2CH_2CH_2CH_3$), 0.83 (t, 6H, ^3J = 5.0 Hz, CH_2CH_3). $^{13}C\{^1H\}$ NMR (125.8 MHz, CD_2Cl_2, 20 °C): δ (ppm) 167.8 (*C*═Pt), 161.4, 159.5 (J_{F-C} = 240 Hz), 132.4, 114.5 (C on Phenyl ring), 125.1 (C≡*C*−Pt), 120.4 and 120.2 (N*C*H═*C*HN), 107.2 and 105.0 (Ph*C*≡*C*−Pt), 63.4 (N*C*H_2N), 50.7, 31.0, 28.6, 22.7, 13.9 (C on the $(CH_2)_4CH_3$). ^{19}F NMR (188.3 MHz, CD_2Cl_2, 20 °C): δ (ppm) −115.8;. ESI^+ MS *m*/*z*: 721.3 (M^+). IR (ART, cm^{-1}) $\nu_{C\equiv C}$ = 2104. Elemental analysis calcd for $C_{33}H_{40}N_4Pt$: C, 54.92; H, 5.03; N, 7.76. Found: C, 55.31; H, 4.90; N, 7.39.

Computational Details. All calculations were performed with the Gaussian 03 program package[38] using the hybrid functional PBE1PBE[39] in conjunction with the Stuttgart/Dresden effective core potentials (SDD) basis set[40] for the Pt center augmented with one f-polarization function (exponent α = 0.993) and the standard 6-31+G(d) basis set[41] for the remaining atoms. Geometry optimizations were performed in the gas phase for both the singlet ground states and the lowest triplet excited states of all complexes. The optimized molecular structures were confirmed to be potential energy minima by vibrational frequency calculations at the same level of theory, as no imaginary frequency was found. The first 10 singlet−singlet and singlet−triplet transition energies were computed at the optimized S_0 geometries by using the time-dependent DFT (TDDFT) methodology.[42−44] Solvent effects were taken into account using the conductor-like polarizable continuum model (CPCM)[45,46] with dichloromethane as a solvent for single-point calculations on all optimized gas-phase geometries.

X-Ray Diffraction Analyses. Intensity data were collected at 183(2) K on an Oxford Xcalibur diffractometer (4-circle kappa platform, Ruby CCD detector, and a single wavelength Enhance X-ray source with MoK_α radiation, λ = 0.71073 Å).[47] The selected suitable single crystals were mounted using polybutene oil on the top of a glass fiber fixed on a goniometer head and immediately transferred to the diffractometer. Pre-experiment, data collection, data reduction, and analytical absorption corrections[48] were performed with the Oxford program suite *CrysAlisPro*.[49] The crystal structures were solved with SHELXS-97[50] using direct methods. The structure refinements were performed by full-matrix least-squares on F^2 with SHELXL-97.[50] All programs used during the crystal structure determination process are included in the WINGX software.[51] The program PLATON[52] was used to check the results of the X-ray analyses. CCDC 787595−787598 contain the supplementary crystallographic data (excluding structure factors) for this paper. These data can be obtained free of charge from The Cambridge Crystallographic Data Centre via www.ccdc.cam.ac.uk/data_request/cif.

Acknowledgment. We thank S. V. Rocha and Dr. N. Finney for help with excited-state lifetime measurements. K.V. is grateful to the University of Zürich and Prof. H. Berke for generous support.

Supporting Information Available: Synthetic protocol of ligand **A**, absorbance spectra of **3** in different solvents, emission spectra of **3** in different solvents, absorbance and emission spectra of **8**, 77 K emission spectra of all complexes, cyclic voltammogram of **8**, and energies and Cartesian coordinates from DFT calculations. This material is available free of charge via the Internet at http://pubs.acs.org.

(42) Bauernschmitt, R.; Ahlrichs, R. *Chem. Phys. Lett.* **1996**, *256*, 454–464.
(43) Casida, M. E.; Jamorski, C.; Casida, K. C.; Salahub, D. R. *J. Chem. Phys.* **1998**, *108*, 4439–4449.
(44) Stratmann, R. E.; Scuseria, G. E.; Frisch, M. J. *J. Chem. Phys.* **1998**, *109*, 8218–8224.
(45) Barone, V.; Cossi, M. *J. Phys. Chem. A* **1998**, *102*, 1995–2001.
(46) Cossi, M.; Rega, N.; Scalmani, G.; Barone, V. *J. Comput. Chem.* **2003**, *24*, 669–681.
(47) *Xcalibur CCD System*; Oxford Diffraction Ltd: Abingdon, England, 2007.
(48) Clark, R. C.; Reid, J. S. *Acta Crystallogr.* **1995**, *51*, 887–897.
(49) *CrysAlisPro*, versions 1.171.32334d-55; Oxford Diffraction Ltd: Abingdon, Oxfordshire, England.
(50) Sheldrick, G. M. *Acta Crystallogr.* **2008**, *64*, 112–122.
(51) Farrugia, L. J. *J. Appl. Crystallogr.* **1999**, *32*, 837.
(52) Spek, A. L. *J. Appl. Crystallogr.* **2003**, *36*, 7–13.